IMPROVEMENT OF THE MELLOR–YAMADA TURBULENCE CLOSURE MODEL BASED ON LARGE-EDDY SIMULATION DATA

MIKIO NAKANISHI*
Japan Weather Association, Toshima, Tokyo 170-6055, Japan

(Received in final form 3 October 2000)

Abstract. On the basis of data constructed with large-eddy simulation (LES), an attempt is made to improve the Mellor–Yamada (M–Y) turbulence closure model. Firstly, stably-stratified and convective planetary boundary layers without moisture are simulated by a LES model to obtain a database for the improvement. Secondly, based on the LES data, closure constants are re-evaluated and a new diagnostic equation for the master length scale L is proposed. The new equation is characterized by allowing L in the surface layer to vary with stability instead of constant kz, where k is the von Kármán constant, and z is height.

The non-dimensional eddy-diffusivity coefficients calculated from the modified M–Ymodel are in satisfactory agreement with those from the LES data. It is found that the modified M–Ymodel improves the original one largely, and that the improvement is achieved by considering buoyancy effects on the pressure covariances andby using the newly proposed equation for L.

Keywords: Closure constant, Eddy-diffusivity coefficient, Large-eddy simulation, Length scale, Level 3 model, Turbulence closure model.

1. Introduction

One of the most important physical processes in the planetary boundary layer (PBL) is turbulence. In the 1970s, several high-order turbulence closure models were developed, and Mellor (1973) and Lewellen and Teske (1973) proposed second-order closure models. Mellor's model was thereafter classified into four hierarchy levels, according to the degree of anisotropy, by Mellor and Yamada (1974), and has been widely applied not only to numerical experiments (e.g., Yamada, 1977; Miyakoda et al., 1983) but also to operational weather forecasts (e.g., Numerical Prediction Division of Japan Meteorological Agency, 1997). Their model is now termed the Mellor–Yamada (M–Y) model.

One of the reasons for the preference of the M–Y model is that it uses a minimum number of universal constants (closure constants) determined from laboratory and field experiments in neutral stratification and yet reproduces nicely the observed non-dimensional gradient functions in the surface layer (Mellor, 1973). However, several problems in the M–Y model have been noted; e.g., Sun

* Current affiliation: National Defence Academy of Japan, Yokosuka, Kanagawa 239-8686, Japan. E-mail: naka@nda.ac.jp

Boundary-Layer Meteorology **99:** 349–378, 2001.

and Ogura (1980) pointed out that the M–Y model underestimates the depth of the mixed layer and destabilizes the stratification in the bulk of the mixed layer.

Three major deficiencies of second-order closure models such as the M–Y model have been mentioned in the literature (e.g., Moeng and Wyngaard, 1989); the first deficiency is the neglect of buoyancy effects on the pressure covariances; the second is the uncertain expression for a length scale, and the third is the downgradient-diffusion assumption for turbulent transports. With respect to the first deficiency, however, Mellor and Yamada (1982) stated that "We use a relatively low-order version of Rotta's 'energy redistribution' hypothesis. Other authors claim some benefit in adding more nonlinear terms; however, our perception is that the benefits are marginal and may even create errors in one application relative to the one in which the additional, requisite, constants were obtained". The aim of the present study is to examine the first two deficiencies, and to improve the M–Y model, based on data constructed with large-eddy simulation (LES).

Turbulence closure models have several unknown parameters to be determined from experiments and/or simulations. Although a large number of observations have been performed in the surface layer and applied to the determination of the unknown parameters, the evaluation of turbulence in stable stratification may be unsatisfactory because of its weakness and the presence of gravity waves. Also, observations throughout the PBL available for the study on turbulence closure modelling, do not exist in sufficient quantity, partly because only a few observational techniques can make such observations.

LES can simulate explicitly turbulent motions whose scale is larger than a grid size. Since the pioneering work of Deardorff (1972), it has been applied to simulations of neutral or convective PBLs and has provided important information on turbulence. A subgrid model proposed by Sullivan et al. (1994) further improved the performance of the LES model in the surface layer and was applied also to a stably-stratified PBL (Andrén, 1995).

In this study we first use a LES model similar to that of Sullivan et al. (1994) (Nakanishi, 2000) to obtain turbulent quantities in dry PBLs with variously stratified conditions. Secondly, we present a M–Y model in which buoyancy effects are incorporated into the parameterization for the pressure covariances. Thereafter, based on the LES data, closure constants are re-evaluated and a new expression for the master length scale is proposed.

2. Construction of LES Database

In the present paper, capital letters denote ensemble-average variables, small letters turbulent variables, the angle brackets $\langle \quad \rangle$ an ensemble average, and a subscript 0 a reference state.

2.1. LES MODEL AND NUMERICAL CONDITIONS

The LES code used here is described in detail in Nakanishi (2000); the moisture and radiation effects, however, are excluded. The subgrid model is similar to that of Sullivan et al. (1994) except that we use a diagnostic equation for the subgrid turbulent kinetic energy (TKE). To simulate steady-state PBL flows, the heat flux $\langle w\theta \rangle_g$ at the ground surface is fixed at a constant value, where w is the vertical velocity component, θ the potential temperature, and the subscript g denotes the ground surface. The surface momentum flux, on the other hand, is determined from Monin–Obukhov theory with the roughness length z_{0m} set at 0.15 m for momentum.

The computational domain consists of 96 × 96 grids horizontally and 60 grids vertically. The lateral boundaries are periodic and the top boundary is treated as a stress-free rigid lid; a grid spacing of either 3 or 4 m is used in all directions and the time step is set to 0.2 s.

According to Canuto and Minotti (1993), the grid spacing has to be smaller than the buoyancy-subrange scale given by $(\pi/\sqrt{6/5})(q^2/2)^{1/2}/N$ if it is used as the length scale, where $q^2/2 \equiv \left\langle u^2 + v^2 + w^2 \right\rangle/2$ is the TKE, $N \equiv \left[(g/\Theta_0)\partial\Theta/\partial z\right]^{1/2}$ the Brunt–Väisälä frequency, g the gravitational acceleration, and (u, v) are the horizontal velocity components. This constraint becomes severe as stability increases. From preliminary runs, and Monin–Obukhov theory for the most stable case, the magnitudes of $q^2/2$ in the surface layer and $\partial\Theta/\partial z$ at a height of z_{0m} were estimated to be about 0.02 m^2 s^{-2} and 0.26 K m^{-1}, respectively; accordingly the buoyancy-subrange scale for our simulations is considered to be more than about 4.4 m. Only for the most stable case, however, the grid spacing of 3 m is adopted for safety's sake. For unstable cases, a larger grid spacing is allowed and a larger computational domain is proper to simulate typical convective PBLs. To unify with simulations for stable cases, however, the grid spacing for unstable cases is also chosen to be 4 m.

By varying $\langle w\theta \rangle_g$, six types of PBL flows were simulated; Cases 1–3 refer to stably-stratified PBLs and Cases 4–6 convective PBLs. To limit the growth of the PBLs, an inversion with a potential-temperature gradient of 0.2 K m^{-1} was placed between 122 and 162 m. The initial profile of the mean potential temperature was uniform (293 K) below the inversion base and had a vertical gradient of 0.004 K m^{-1} above the inversion top. The mean wind was initially geostrophic and was everywhere equal to 2 m s^{-1}. For Cases 1–3, however, these profiles were replaced by those close to a steady state obtained from a M–Y model (Mellor and Yamada, 1982) in order to reduce the calculation time. The simulations were initialized by adding small random perturbations to the above profiles.

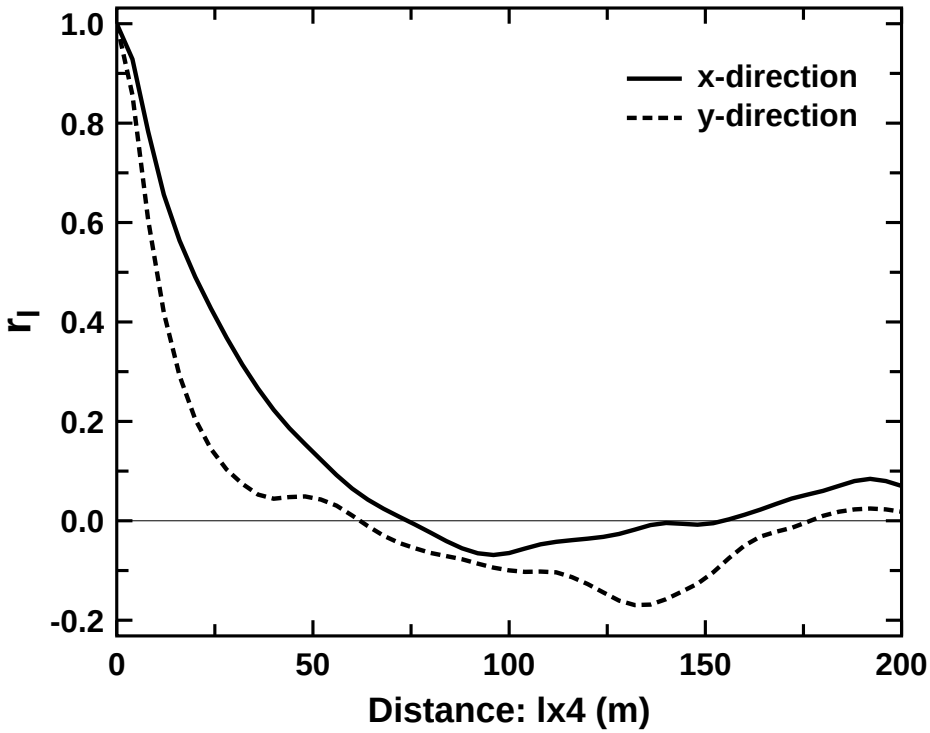

Figure 1. Two-point correlation r_l of the horizontal velocity component at the centre of the PBL ($z = 70$ m) for Case 6. The solid and dashed lines represent r_l for the x-direction (parallel to the geostrophic wind) and y-direction, respectively. Only about a half of the computational-domain size is shown, since the other half is the same.

2.2. RESULTS

In order to justify the choice of the computational domain, Figure 1 shows two-point correlation r_l of the horizontal velocity component u: e.g., for the x-direction (parallel to the geostrophic wind),

$$r_l = \frac{\sum_{i=1}^{96}\sum_{j=1}^{96} u_{i,j}u_{i+l,j}}{\sum_{i=1}^{96}\sum_{j=1}^{96} u_{i,j}^2}, \quad 0 \le l < 96 \tag{1}$$

at the centre of the PBL for Case 6 with the largest PBL depth. r_l for both the x- and y-directions decreases exponentially with increasing l, and its absolute value for large l settles down to less than about 0.1; accordingly the choice of the computational domain is considered to be allowable.

TABLE I

Input and output parameters for the LESs. Δ is the grid spacing, τ_* the large-eddy turnover time, and L_M the Obukhov length. Time averaging is made over a period of 30 minutes after the simulations are run for about 10 τ_*.

Case	Δ (m)	$\langle w\theta \rangle_g$ (K m s^{-1})	h, z_i (m)	u_* (m s^{-1})	w_* (m s^{-1})	τ_* (s)	h/L_M, z_i/L_M
1	3	–0.001	69	0.074	–	927	2.24
2	4	–0.0006	100	0.084	–	1187	1.34
3	4	–0.0003	116	0.092	–	1260	0.60
4	4	0.003	128	0.108	0.234	547	–4.05
5	4	0.01	132	0.116	0.353	374	–11.25
6	4	0.025	140	0.124	0.489	286	–24.37

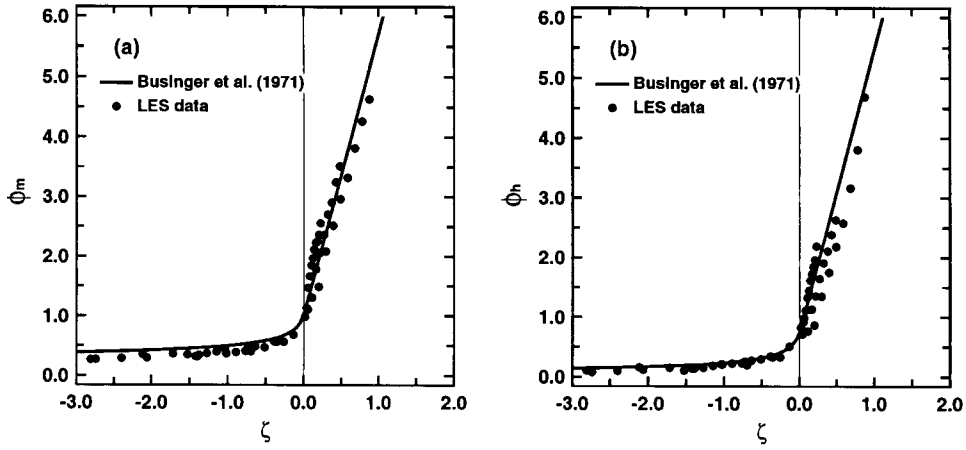

Figure 2. Comparison of (a) ϕ_m and (b) ϕ_h calculated from the LES data with the empirical functions. Full circles show the LES results ($z/h < 0.4$ for Cases 1–3 and $z/z_i < 0.4$ for Cases 4–6) and solid lines the empirical functions by Businger et al. (1971) (Appendix A).

The statistical quantities are obtained by averaging over a horizontal plane and over a period of 30 min after a statistically quasi-steady state is reached. The quasi-steady state may be reached within a few large-eddy turnover times, where one large-eddy turnover time is given by h/u_* for Cases 1–3 and z_i/w_* for Cases 4–6; here, u_* is the friction velocity, $w_* \equiv \left[(g/\Theta_0)\langle w\theta \rangle_g z_i\right]^{1/3}$ the convective velocity, and h and z_i are the depths of the stably-stratified and convective PBLs, respectively. Note that h is defined as the height where the buoyancy flux falls to 5% of its surface value, while z_i is the height where the buoyancy flux is minimum. The input parameters and the resulting statistics are summarized in Table I.

To verify the reliability of the LES data, Figure 2 compares $\phi_m(\zeta)$ and $\phi_h(\zeta)$ calculated from the LES data with those experimentally obtained by Businger et al. (1971) (Appendix A). ϕ_m and ϕ_h are the non-dimensional gradient functions for momentum and heat, respectively, and are given by

$$\phi_m = \frac{kz}{u_*}\left[\left(\frac{\partial U}{\partial z}\right)^2 + \left(\frac{\partial V}{\partial z}\right)^2\right]^{1/2}, \tag{2}$$

$$\phi_h = \frac{kz}{\theta_*}\frac{\partial \Theta}{\partial z}, \tag{3}$$

where k is the von Kármán constant and θ_* the scaling temperature. $\zeta \equiv z/L_M$ is the non-dimensional height normalized by the Obukhov length L_M:

$$L_M = -\frac{\Theta_0 u_*^3}{kg\langle w\theta\rangle_g}. \tag{4}$$

Although the depth of the surface layer is considered to be about 10% of the PBL depth, the LES data are plotted for $0 < z < 0.4h$ or $0.4z_i$. For Cases 4–6 ($\zeta < 0$), both ϕ_m and ϕ_h computed from the LES data are in good agreement with the empirical functions. For Cases 1–3 ($\zeta > 0$), however, they fluctuate slightly around the empirical functions. The difference between the LES results and the empirical functions is especially large for ϕ_h in Case 1, which is for the most stable condition (Figure 2b). Since the form of ϕ_h experimentally determined so far varies considerably (e.g., Yaglom, 1977), however, the present LES data are considered to reproduce the properties of the surface layer satisfactorily.

3. Description of the Mellor–Yamada Model

3.1. Parameterization

In second-order closure models such as the M–Y model, the dissipation rates, the pressure covariances, and the third moments are parameterized. Mellor (1973) expressed the dissipation rates of TKE $q^2/2$ and temperature variance $\langle\theta^2\rangle$ as

$$\varepsilon = \frac{q^3}{B_1 L}, \tag{5}$$

$$\varepsilon_\theta = \frac{q}{B_2 L}\langle\theta^2\rangle, \tag{6}$$

respectively, where L is the turbulent master length scale, and B_1 and B_2 are the closure constants.

On the other hand, the pressure-strain and pressure-temperature-gradient covariances are usually parameterized as

$$\left\langle p\left(\frac{\partial u_i}{\partial x_j}+\frac{\partial u_j}{\partial x_i}\right)\right\rangle = -\frac{q}{3A_1L}\left(\langle u_iu_j\rangle-\frac{1}{3}q^2\delta_{ij}\right) + C_1q^2\left(\frac{\partial U_i}{\partial x_j}+\frac{\partial U_j}{\partial x_i}\right) - C_2\frac{g}{\Theta_0}\left(\langle u_i\theta\rangle\,\delta_{j3}+\langle u_j\theta\rangle\,\delta_{i3}-\frac{2}{3}\langle u_3\theta\rangle\,\delta_{ij}\right) + C_4\left(\langle u_iu_k\rangle\frac{\partial U_j}{\partial x_k}+\langle u_ju_k\rangle\frac{\partial U_i}{\partial x_k}-\frac{2}{3}\langle u_ku_l\rangle\frac{\partial U_k}{\partial x_l}\delta_{ij}\right), \tag{7}$$

$$\left\langle p\frac{\partial\theta}{\partial x_i}\right\rangle = -\frac{q}{3A_2L}\langle u_i\theta\rangle - C_3\frac{g}{\Theta_0}\langle\theta^2\rangle\delta_{i3} + C_5\langle u_k\theta\rangle\frac{\partial U_i}{\partial x_k}, \tag{8}$$

respectively (e.g., Denby, 1999), where u_i is the velocity vector, p the pressure divided by the mean density, and A and C with subscripts are also the closure constants. The terms with C_1, C_4, or C_5 and those with C_2 or C_3 represent effects of shear and buoyancy, respectively, and are neglected in Mellor (1973) except for the term with C_1. Although these terms are likely to be effective for the parameterization for the pressure covariances as suggested by Moeng and Wyngaard (1986) and Andrén and Moeng (1993), it is found that the term with C_4 (in this formulation) has a contrary effect on the reproduction of the horizontal velocity variance given by our LES data. Since shear effects are considered through the term with C_1, we will adopt $C_4 = 0$.

As for the parameterization for the third moments, it is especially important in the convective PBL but is not discussed in the present paper.

Based on several measurements, Mellor and Yamada (1982) estimated the closure constants as

$$\begin{aligned}(A_1, A_2, B_1, B_2, C_1) &= (0.92, 0.74, 16.6, 10.1, 0.08),\\ (C_2, C_3, C_4, C_5) &= (0, 0, 0, 0).\end{aligned} \tag{9}$$

3.2. Expression in the surface layer

If the boundary-layer approximation is applied and the time-tendency, advection, and diffusion terms are neglected (Level 2 model; Mellor and Yamada, 1974, 1982), the variances and the turbulent fluxes are written as

$$\langle u^2\rangle = \gamma_1q^2 + 2A_1C_2\frac{L}{q}\frac{g}{\Theta_0}\langle w\theta\rangle - 6A_1\frac{L}{q}\langle uw\rangle\frac{\partial U}{\partial z}, \tag{10}$$

$$\langle v^2\rangle = \gamma_1q^2 + 2A_1C_2\frac{L}{q}\frac{g}{\Theta_0}\langle w\theta\rangle, \tag{11}$$

$$\langle w^2\rangle = \gamma_1q^2 + 2A_1(3-2C_2)\frac{L}{q}\frac{g}{\Theta_0}\langle w\theta\rangle, \tag{12}$$

$$\langle uw\rangle = 3A_1\frac{L}{q}\left[-\left(\langle w^2\rangle - C_1q^2\right)\frac{\partial U}{\partial z} + (1-C_2)\frac{g}{\Theta_0}\langle u\theta\rangle\right], \tag{13}$$

$$\langle u\theta\rangle = 3A_2\frac{L}{q}\left[-\langle uw\rangle\frac{\partial \Theta}{\partial z} - (1-C_5)\,\langle w\theta\rangle\frac{\partial U}{\partial z}\right], \tag{14}$$

$$\langle w\theta\rangle = 3A_2\frac{L}{q}\left[-\langle w^2\rangle\frac{\partial \Theta}{\partial z} + (1-C_3)\,\frac{g}{\Theta_0}\langle\theta^2\rangle\right], \tag{15}$$

$$q^2 = B_1\frac{L}{q}\left(-\langle uw\rangle\frac{\partial U}{\partial z} + \frac{g}{\Theta_0}\langle w\theta\rangle\right), \tag{16}$$

$$\langle\theta^2\rangle = -\,B_2\frac{L}{q}\langle w\theta\rangle\frac{\partial \Theta}{\partial z}, \tag{17}$$

where the coordinate system is oriented so that $\langle vw\rangle = 0$, and $\gamma_1 \equiv 1/3 - 2A_1/B_1$.

Substitution of the relationships in the surface layer:

$$\begin{aligned} &\langle uw\rangle = -u_*^2, \quad \langle w\theta\rangle = -u_*\theta_*, \quad \zeta = z/L_M, \\ &\frac{\partial U}{\partial z} = \frac{u_*}{kz}\phi_m, \quad \frac{\partial \Theta}{\partial z} = \frac{\theta_*}{kz}\phi_h \end{aligned} \tag{18}$$

into the above equations gives some non-dimensional variables:

$$\frac{q^3}{u_*^3} \equiv q^{*3} = B_1\frac{L}{kz}\,(\phi_m - \zeta)\,, \tag{19}$$

$$\frac{\langle u^2\rangle}{q^2} = \gamma_1 + \left(\frac{1}{3} - \gamma_1\right)\frac{3\phi_m - C_2\zeta}{\phi_m - \zeta}, \tag{20}$$

$$\frac{\langle\theta^2\rangle}{\theta_*^2} = \left(\frac{L}{kz}\right)^{2/3}\frac{B_2}{B_1^{1/3}}\frac{\phi_h}{(\phi_m - \zeta)^{1/3}}, \tag{21}$$

$$\frac{\langle u\theta\rangle}{u_*\theta_*} = \left(\frac{L}{kz}\right)^{2/3}\frac{3A_2}{B_1^{1/3}}\frac{(1-C_5)\phi_m + \phi_h}{(\phi_m - \zeta)^{1/3}} \tag{22}$$

and simultaneous equations for the non-dimensional gradient functions, ϕ_m and ϕ_h:

$$\begin{aligned} \phi_m\left\{\gamma_1 - C_1 - [2A_1(3-2C_2) + 3A_2(1-C_2)(1-C_5)]\,\frac{\zeta}{q^{*3}}\frac{L}{kz}\right\} \\ - \phi_h\left[3A_2(1-C_2)\frac{\zeta}{q^{*3}}\frac{L}{kz}\right] = \frac{1}{3A_1q^*}\frac{kz}{L}, \end{aligned} \tag{23}$$

$$\phi_h\left\{\gamma_1 - [2A_1(3-2C_2) + B_2(1-C_3)]\,\frac{\zeta}{q^{*3}}\frac{L}{kz}\right\} = \frac{1}{3A_2q^*}\frac{kz}{L}. \tag{24}$$

In addition, since $\phi_m = 1$, $\phi_h = Pr$, and $L = kz$ in neutral stratification ($\zeta = 0$), we obtain

$$A_1 = B_1\frac{1-3\gamma_1}{6}, \quad A_2 = \frac{1}{3\gamma_1B_1^{1/3}Pr}, \quad C_1 = \gamma_1 - \frac{1}{3A_1B_1^{1/3}}, \tag{25}$$

where Pr is the turbulent Prandtl number.

3.3. LEVEL 3 MODEL

In the Level 3 model (Mellor and Yamada, 1974, 1982), the TKE $q^2/2$ and the temperature variance $\langle\theta^2\rangle$ are predicted by applying prognostic equations, while the other turbulent variables are solved diagnostically as given by Equations (10)–(15). The equations for the velocity variances, however, are changed by eliminating q^2/B_1, which is the term associated with the dissipation, using Equation (16); e.g., the equation for the vertical velocity variance $\langle w^2\rangle$ is

$$\langle w^2\rangle = \frac{q^2}{3} + 2A_1\frac{L}{q}\langle uw\rangle\frac{\partial U}{\partial z} + 4A_1(1-C_2)\frac{L}{q}\frac{g}{\Theta_0}\langle w\theta\rangle \tag{26}$$

instead of Equation (12).

We will define non-dimensional variables:

$$\begin{aligned}
G_M &= \frac{L^2}{q^2}\left(\frac{\partial U}{\partial z}\right)^2, \quad G_H = -\frac{L^2}{q^2}\frac{g}{\Theta_0}\frac{\partial \Theta}{\partial z},\\
C_w &= \langle w^2\rangle/q^2, \quad C_\theta = \langle\theta^2\rangle \Big/ L^2\left(\frac{\partial \Theta}{\partial z}\right)^2,\\
T_u &= \langle u\theta\rangle \Big/ L^2\frac{\partial U}{\partial z}\frac{\partial \Theta}{\partial z},\\
S_M &\equiv S_{M2.5} + S'_M = -\langle uw\rangle \Big/ Lq\frac{\partial U}{\partial z},\\
S_H &\equiv S_{H2.5} + S'_H = -\langle w\theta\rangle \Big/ Lq\frac{\partial \Theta}{\partial z},
\end{aligned} \tag{27}$$

where a subscript 2.5 denotes a variable in the Level 2.5 model (Yamada, 1977; Mellor and Yamada, 1982) and a prime the fluctuation from it. In the Level 2.5 model, $\langle\theta^2\rangle$ is also solved diagnostically using Equation (17). Substitution of these variables into Equations (13)–(15), (17), and (26) gives

$$\begin{aligned}
&C_{\theta 2.5} = B_2 S_{H2.5},\\
&C_w = 1/3 - 2A_1 G_M S_M + 4A_1(1-C_2)G_H S_H,\\
&T_u = 3A_2\left[S_M + (1-C_5)S_H\right],\\
&S_M = 3A_1\left[C_w - C_1 + (1-C_2)G_H T_u\right],\\
&S_H = 3A_2\left[C_w + (1-C_3)G_H C_\theta\right].
\end{aligned} \tag{28}$$

After some algebra, the non-dimensional eddy-diffusivity coefficients, $S_{M2.5}$, $S_{H2.5}$, S'_M, and S'_H, reduce to

$$S_{M2.5} = \frac{A_2E_2 - R_1E_4}{E_2E_3 - E_1E_4}, \qquad S'_M = \frac{R'_2E_2}{E_2E_3 - E_1E'_4}, \tag{29}$$

$$S_{H2.5} = \frac{R_1E_3 - A_2E_1}{E_2E_3 - E_1E_4}, \qquad S'_H = \frac{-R'_2E_1}{E_2E_3 - E_1E'_4}, \tag{30}$$

where

$$\begin{aligned}
E_1 &= 1 + 6A_1^2G_M - 9A_1A_2(1 - C_2)G_H,\\
E_2 &= -3A_1\,[4A_1 + 3A_2(1 - C_5)]\,(1 - C_2)G_H,\\
E_3 &= 6A_1A_2G_M,\\
E'_4 &= 1 - 12A_1A_2(1 - C_2)G_H,\\
E_4 &= E'_4 - 3A_2B_2(1 - C_3)G_H,\\
R_1 &= A_1(1 - 3C_1),\\
R'_2 &= 3A_2(1 - C_3)G_H(C_\theta - B_2S_{H2.5}).
\end{aligned} \tag{31}$$

The Level 2.5 model is known to behave pathologically for growing turbulence. Helfand and Labraga (1988) modified the Level 2.5 model so as to ensure its realizability (Schumann, 1977) and to remove its pathological behaviour; when TKE $q^2/2$ is smaller than TKE $q_2^2/2$ predicted by the Level 2 model, i.e., in the case of growing turbulence, $S_{M2.5}$ and $S_{H2.5}$ are replaced by $S_{M2} \times q/q_2$ and $S_{H2} \times q/q_2$, respectively. In addition to these modifications, $C_\theta - B_2S_{H2.5}$ in Equation (31) is changed for

$$C_\theta - \frac{q}{q_2}B_2S_{H2.5} = C_\theta - \frac{q^2}{q_2^2}B_2S_{H2}. \tag{32}$$

S_{M2} and S_{H2} are specified in Appendix B.

Since Helfand and Labraga (1988) paid attention to the Level 2.5 model, they expressed no idea for modifications of S'_M and S'_H. Characteristics of the Level 3 model may also need to be examined, for example, with a scheme similar to that of Gerrity et al. (1994).

4. Evaluation of the Closure Constants and the Length Scale

4.1. Length scale in the surface layer

Mellor (1973) assumed that the master length scale L in the surface layer is given by kz regardless of stability. According to some observations, however, L varies with stability (Busch and Larsen, 1972). Dubrulle and Niino (1992) reported that, in the M–Y model, the normalized TKE given by Equation (19) with $L = kz$ increases infinitely as stability increases, and that this shortcoming can be improved

by considering the dependence of L on stability. Here we will first examine L in the surface layer based on the LES data.

In the M–Y model, L is representative of both the diffusion and dissipation length scales. In the convective PBL the diffusion length scale is not easy to determine accurately, since the vertical gradient of physical quantities is small. Thus we will evaluate the dissipation length scale.

The dissipation ε of the TKE is parameterized as Equation (5). If a local-equilibrium state of the TKE in the surface layer is assumed (Equation (19)), we obtain

$$B_1 \frac{L}{kz} \left(= \frac{q^3}{\varepsilon\, kz} \right) = \frac{q^3}{u_*^3} \frac{1}{\phi_m - \zeta}. \tag{33}$$

The LES computes ε, the TKE $q^2/2$, and the friction velocity u_* as a total of the resolved-scale and subgrid-scale quantities. First, these quantities at several height levels were substituted into $q^3/\varepsilon\, kz$ and the resulting non-dimensional length scale $B_1 L/kz$ was plotted against the non-dimensional height ζ. The plotted points for the stable cases seem to lie nearly in a single curve but with some scatter (not shown). This scatter is perhaps because the turbulent transports of $q^2/2$ and ε exist a little even in stable conditions. Instead of such a plot, shown in Figure 3 is the plot of $B_1 L/kz$ in Equation (33), where the non-dimensional gradient function ϕ_m is given by the empirical function by Businger et al. (1971).

Figure 3 demonstrates that L varies with stability and that $B_1 L/kz$ for Cases 1–3 ($\zeta > 0$) is approximated by a curve:

$$B_1 \frac{L}{kz} = 24.0(1 + 2.7\zeta)^{-1}. \tag{34}$$

Since $L = kz$ in neutral stratification ($\zeta = 0$), $B_1 = 24.0$ and L in stable stratification becomes

$$L \equiv L_S = kz(1 + 2.7\zeta)^{-1} \quad \text{for} \quad \zeta \geq 0. \tag{35}$$

This value of B_1 is somewhat larger than 16.6 estimated by Mellor and Yamada (1982), but is close to 27.4 obtained from their LES by Andrén and Moeng (1993) and 22.6 used by Therry and Lacarrère (1983).

On the other hand, $B_1 L/kz$ for Cases 4–6 ($\zeta < 0$) shows a large scatter. Although $B_1 L/kz$ tends to increase with decreasing ζ, its increasing curve depends upon the height. This may be because the turbulent transport throughout the convective mixed layer has a significant influence also on the surface layer. In the Level 2 version used for the analysis of the surface layer (see Section 3.2), all the turbulent diffusions are neglected; accordingly the contribution of the turbulent diffusion to L should be also removed here. Since it cannot be estimated from the present LES data, however, L in unstable stratification is assumed to be given by kz for simplicity.

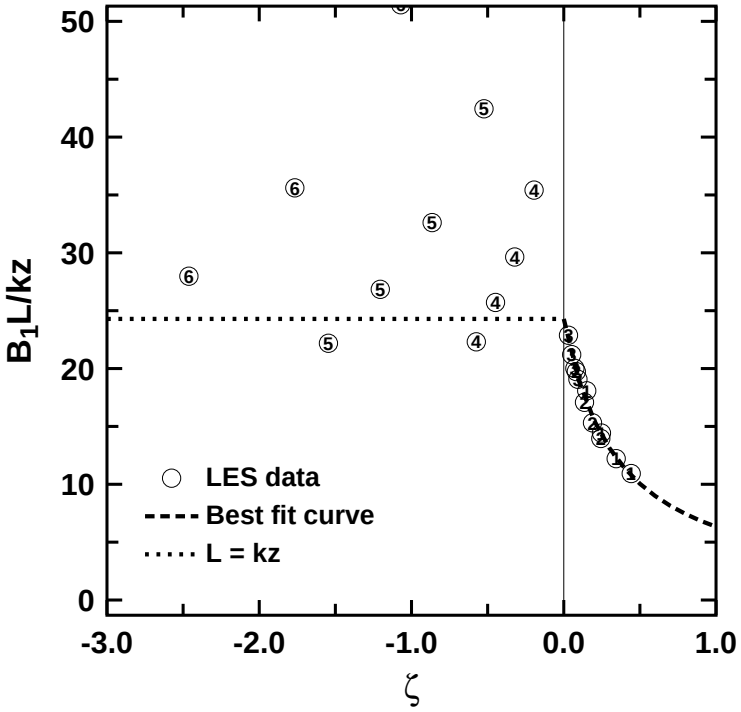

Figure 3. Plot of $B_1 L/kz$ as a function of ζ. A number in a circle indicates the case number in Table I. The LES results are plotted only between the second (4.5 or 6 m) and fifth (13.5 or 18 m) grid points above the ground surface, which are considered to be nearly in the surface layer. The dashed line represents the best fit curve for Cases 1–3 and the dotted line the line of $L = kz$.

4.2. CLOSURE CONSTANTS

The closure constants can be evaluated by comparing the non-dimensional variables in the surface layer, given by Equations (20)–(22), with those calculated from the LES data. The non-dimensional gradient functions, ϕ_m and ϕ_h, are derived from Equations (19), (23), (24), (35), and $L = kz$ for $\zeta < 0$, by an iterative procedure.

In order to obtain the total (resolved-scale plus subgrid-scale) temperature variance $\langle\theta^2\rangle$ in the LES, the subgrid temperature variance $\overline{\theta''^2}$ was given by

$$\overline{\theta''^2} = \frac{2l}{c_\theta e^{1/2}} \left(-\overline{u_j''\theta''} \frac{\partial \overline{\theta}}{\partial x_j} \right), \tag{36}$$

where an overbar denotes a resolved-scale variable, a double prime a subgrid-scale variable, e is the subgrid TKE, and l the length scale set equal to the grid spacing (Nakanishi, 2000). A constant c_θ was taken to be 2.1 as in Moeng and Wyngaard (1988).

Figure 4 shows plots of $\langle u^2\rangle/q^2$, $\langle\theta^2\rangle/\theta_*^2$, and $\langle u\theta\rangle/u_*\theta_*$ at four height levels, computed from the LES data. Since the LES results illustrate that $\langle u^2\rangle/q^2$ at $\zeta = 0$

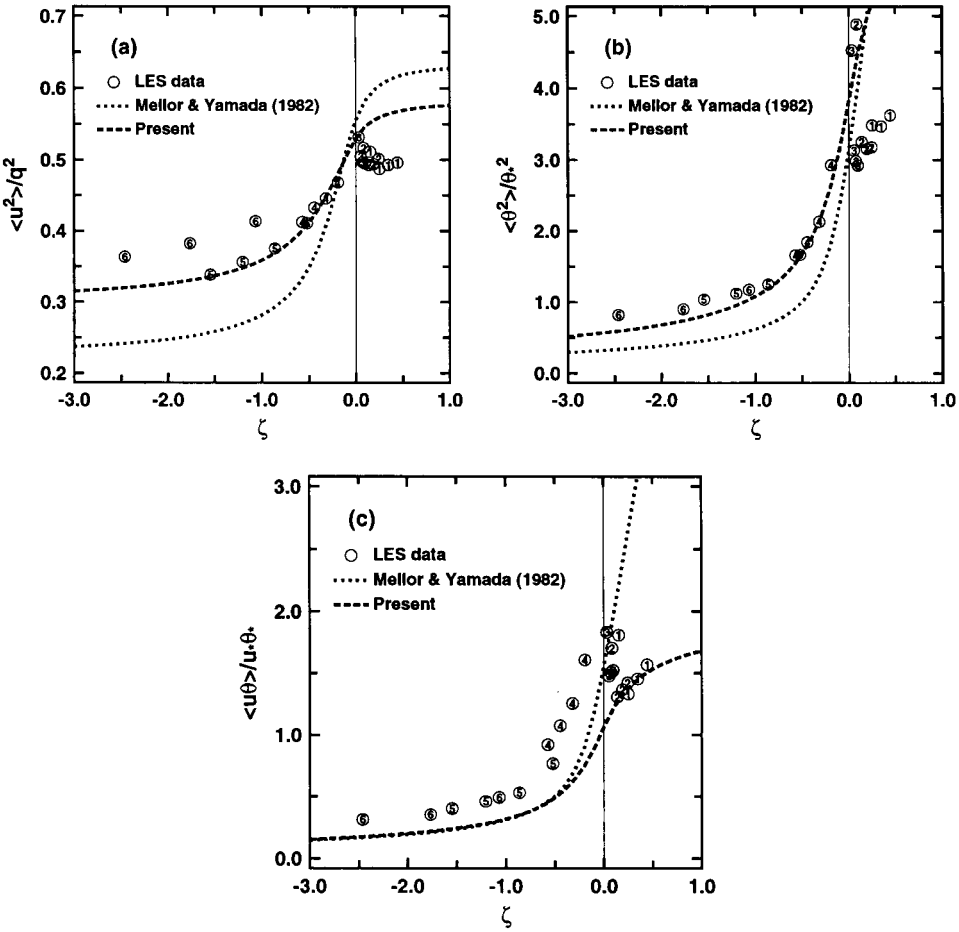

Figure 4. Plots of (a) $\langle u^2\rangle/q^2$, (b) $\langle\theta^2\rangle/\theta_*^2$, and (c) $\langle u\theta\rangle/u_*\theta_*$ as a function of ζ. The dashed line in (a) represents Equation (20) with $\gamma_1 = 0.235$ and $C_2 = 0.65$, that in (b) Equation (21) with $B_1 = 24.0$, $B_2 = 15.0$, and $Pr = 0.74$, and that in (c) Equation (22) with $A_2 = 0.665$ and $C_5 = 0.2$, where ϕ_m and ϕ_h are derived from Equations (19), (23), and (24), and L is given by Equation (35) and kz for $\zeta < 0$. Others are the same as in Figure 3. For reference, dotted lines show the corresponding equations with the original closure constants (Equation (9)) and $L = kz$.

($= 1 - 2\gamma_1$ in Equation (20)) is nearly equal to 0.53, we obtain $\gamma_1 \approx 0.235$ (Figure 4a). The results of the M–Y model with modified closure constants (dashed line) nearly coincide with those of the LES, where a selected value of $C_2 = 0.65$ is the same as that of Gambo (1978).

Since the magnitude of $\langle\theta^2\rangle/\theta_*^2$ at $\zeta = 0$ ($= B_2 Pr/B_1^{1/3}$ in Equation (21) with $\phi_m = 1$, $\phi_h = Pr$, and $L = kz$) is difficult to determine from the LES results, we choose values of $Pr = 0.74$ and $B_2 = 15.0$ so that, for the unstable cases, the results of a modified M–Y model (dashed line) may agree with those of the LES

(Figure 4b). The resulting value of $B_2/B_1 = 0.625$ is very close to that of Mellor and Yamada (1982).

With the closure constants determined above and Equation (25), the magnitude of $\langle u\theta\rangle/u_*\theta_*$ at $\zeta = 0$ ($= 3A_2(1-C_5+Pr)/B_1^{1/3}$ in Equation (22)) is smaller than 1.2 as long as C_5 is positive, and is somewhat smaller than that of the LES results (Figure 4c). With respect to its magnitude near $\zeta = 0$, the original M–Y model (dotted line) makes a better prediction mainly because of the smaller value of B_1 (see Equation (9)). However, the original M–Y model has a defect that $\langle u\theta\rangle/u_*\theta_*$ increases infinitely with increasing ζ. Since Andrén and Moeng (1993) concluded that shear effects, which are parameterized as the term with C_5 for the pressure-temperature-gradient covariance, must be included in any model, C_5 is chosen to be 0.2 so that the results of a modified M–Y model (dashed line) may not become worse than those of the original M–Y model.

Finally, C_3 is selected to be 0.294 so that ϕ_h derived from Equations (23) and (24) may approach 4.7ζ as $\zeta \to +\infty$ as in Businger et al. (1971). The resulting ϕ_m approaches 5.11ζ as $\zeta \to +\infty$. It is mentioned that the asymptotic line at $\approx 4.7\zeta$ is inadequate for large ζ (e.g., Beljaars and Holtslag, 1991). The present model, however, does not allow us to adopt their proposed asymptotic line ($\phi_m \to \zeta$ and $\phi_h \sim \zeta^{3/2}$), since it requires that, as stability increases, ϕ_m should approach $a\zeta$ with $a > 1.0$ and ϕ_h should be proportional to ζ.

Although Figure 3 suggests that the turbulent diffusion under unstable conditions is important even in the surface layer, it is neglected in the Level 2 version (see Section 3.2); nevertheless, the modified M–Y model reproduces the LES results reasonably well. We believe that, fortunately, the height variation of the non-dimensional length scale B_1L/kz nearly cancels the contribution of the turbulent diffusion.

In summary, the LES data give a revised set of the closure constants as

$$\begin{aligned}(A_1, A_2, B_1, B_2, C_1) &= (1.18, 0.665, 24.0, 15.0, 0.137),\\ (C_2, C_3, C_4, C_5) &= (0.65, 0.294, 0.0, 0.2).\end{aligned} \tag{37}$$

Consequently the modified M–Y model predicts a critical flux Richardson number of 0.279 (Equation (B5) in Appendix B).

4.3. Diagnostic equation for the length scale

The determination of the master length scale L is one of the most difficult problems in turbulence closure modelling. Although an attempt has been made to evaluate L using a prognostic equation (e.g., Mellor and Yamada, 1982), such an equation is still of a qualitative nature with little physical foundation. In fact, if their equation is incorporated into a Level 4 model (Mellor and Yamada, 1974, 1982) and applied to the surface layer, one cannot obtain solutions for very unstable and very stable conditions (Niino, 1990).

Numerous diagnostic equations for L have been proposed in the literature. As shown by Therry and Lacarrère (1983), however, several diagnostic equations give L considerably different from each other. This is considered to be due partly to the variety of turbulence closure modelling, but mainly to the lack of data available for the formulation for such an equation.

Since the present LES data cover a relatively wide range of stability, a more general equation for L is expected to be formulated. We propose a new diagnostic equation for L that consists of three length scales, L_S, L_T, and L_B, i.e.,

$$\frac{1}{L} = \frac{1}{L_S} + \frac{1}{L_T} + \frac{1}{L_B}, \tag{38}$$

where L_S is the length scale in the surface layer as obtained in Section 4.1, L_T the length scale depending upon the turbulent structure of the PBL (Mellor and Yamada, 1974), and L_B the length scale limited by the buoyancy effect. This expression is designed in order that the shortest length (or time) scale may control L. L_S, L_T, and L_B are given by

$$L_S = \begin{cases} kz/3.7, & \zeta \geq 1 \\ kz(1+2.7\zeta)^{-1}, & 0 \leq \zeta < 1 \\ kz(1-\alpha_4\zeta)^{0.2}, & \zeta < 0, \end{cases} \tag{39}$$

$$L_T = \alpha_1 \frac{\int_0^\infty qz\,dz}{\int_0^\infty q\,dz}, \tag{40}$$

$$L_B = \begin{cases} \alpha_2 q/N, & \partial\Theta/\partial z > 0 \text{ and } \zeta \geq 0 \\ \left[\alpha_2 q + \alpha_3 q(q_c/L_T N)^{1/2}\right]/N, & \partial\Theta/\partial z > 0 \text{ and } \zeta < 0 \\ \infty, & \partial\Theta/\partial z \leq 0, \end{cases} \tag{41}$$

where α_1, α_2, α_3, and α_4 are empirical constants, and $q_c \equiv \left[(g/\Theta_0)\langle w\theta\rangle_g L_T\right]^{1/3}$ is a velocity scale similar to the convective velocity w_*.

Unlike L_S in Equation (35), we adopt $L_S = kz/3.7$ in the range of $\zeta \geq 1$, partly because the adequacy of L_S is not examined in very stable conditions (see Figure 3) and partly because L without this limit is found to cause excessive dissipation of TKE in a test one-dimensional simulation. Also L_S for $\zeta < 0$ is assumed to be given by $kz(1-\alpha_4\zeta)^{0.2}$ instead of kz by considering effects of the turbulent transport throughout the convective PBL, where a power of 0.2 is determined from the variation of L_S with ζ at the same height in Figure 3. This functional form is arbitrary. L_S for $\zeta < 0$ is also estimated to be a function of ζ, however, since the observed and simulated non-dimensional gradient functions normalized by the length scale of kz lie nearly on a single curve against ζ (see Figure 2).

The expression q/N for L_B is considered to underestimate a length scale in the upper part of the convective PBL, since it is obtained from the balance between

the TKE and the potential energy without considering the increase of TKE due to the turbulent transport and the buoyancy production. According to Moeng and Sullivan (1994), in the highly convective PBL, the sum of the increase rates of TKE due to the turbulent transport and the buoyancy production is nearly proportional to w_*^3/z_i. If the time scale is assumed to be N^{-1}, the increase of TKE is proportional to $w_*^3/z_i N$. Above the convective PBL, however, it must decrease gradually to zero with increasing height. Thus we will tentatively replace $w_*^3/z_i N$ by $q^2 w_*/z_i N$, since q^2 is expected to be nearly uniform owing to the uniform production w_*^3/z_i below z_i and decreases gradually to zero above z_i. When q_c and L_T are used instead of w_* and z_i, respectively, we obtain the expression $q^2 q_c/L_T N$ in Equation (41).

The empirical constants are determined by tuning L obtained from the new equation to that from the LES data ($L = q^3/B_1\varepsilon$; see Equation (5)). While noting $\alpha_2 \leq 1.0$, we first adopt $\alpha_1 = 0.23$ and $\alpha_2 = 1.0$ through the tuning for Cases 1–3. Secondly, $\alpha_3 = 5.0$ and $\alpha_4 = 100.0$ are determined from the tuning near the PBL top ($z = z_i$) and the surface, respectively, for Cases 4–6. The value of $\alpha_1 = 0.23$ falls within the range of 0.20–0.25 estimated for a neutral PBL by Andrén (1991), and is close to 0.2 suggested using a prognostic equation for $q^2 L$ by Mellor (personal communication quoted from Moeng and Wyngaard, 1989).

Figure 5 compares L obtained from the new equation with the LES results. L in the LES becomes very large above h or z_i, since ε of the denominator becomes nearly equal to zero there. For reference, L computed from a diagnostic equation by Therry and Lacarrère (1983) (Appendix C) is shown by dotted lines. Although the form of our equation is simpler than that of Therry and Lacarrère's equation, L from our equation is in better agreement with the LES results except for Case 1 (Figure 5a). The major factor of the simpler form consists in L_S varying with stability and that of the better agreement lies in L_B involving the effect of the increase of TKE in the convective PBL.

5. Verification of the Modified Mellor–Yamada Model

5.1. ϕ_m AND ϕ_h

In order to examine the performance of the M–Y model after the modification of the closure constants, we will first compare the non-dimensional gradient functions for momentum and heat, ϕ_m and ϕ_h, derived from Equations (23) and (24) with the empirical functions by Businger et al. (1971).

Figure 6 shows ϕ_m and ϕ_h before and after that modification and the empirical functions. In stable conditions ($\zeta > 0$), both ϕ_m and ϕ_h before and after the modification are in good accordance with the empirical functions. In unstable conditions ($\zeta < 0$), ϕ_h after the modification agrees very well with the empirical function (Figure 6b). ϕ_m after the modification is also improved considerably compared with ϕ_m before the modification (Figure 6a), although it remains slightly smaller

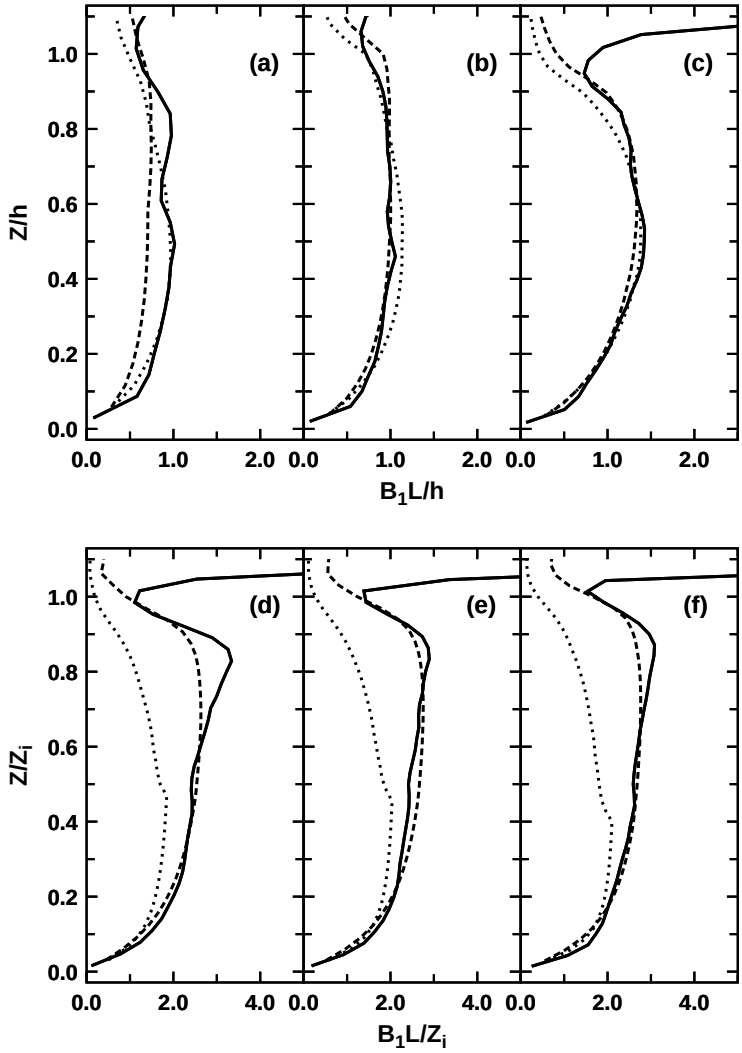

Figure 5. Vertical profiles of L for (a) Case 1, (b) Case 2, (c) Case 3, (d) Case 4, (e) Case 5, and (f) Case 6. Solid lines represent L obtained from the LES data, dashed lines L from Equations (38)–(41) with $\alpha_1 = 0.23$, $\alpha_2 = 1.0$, $\alpha_3 = 5.0$, and $\alpha_4 = 100.0$, and dotted lines L from the equation by Therry and Lacarrère (1983) (Appendix C). The altitude is normalized by h for Cases 1–3 (a–c) and z_i for Cases 4–6 (d–f).

than the empirical function. As will be shown in the following section, it is found that the improvement of ϕ_m and ϕ_h depends upon the consideration of buoyancy effects on the pressure covariances.

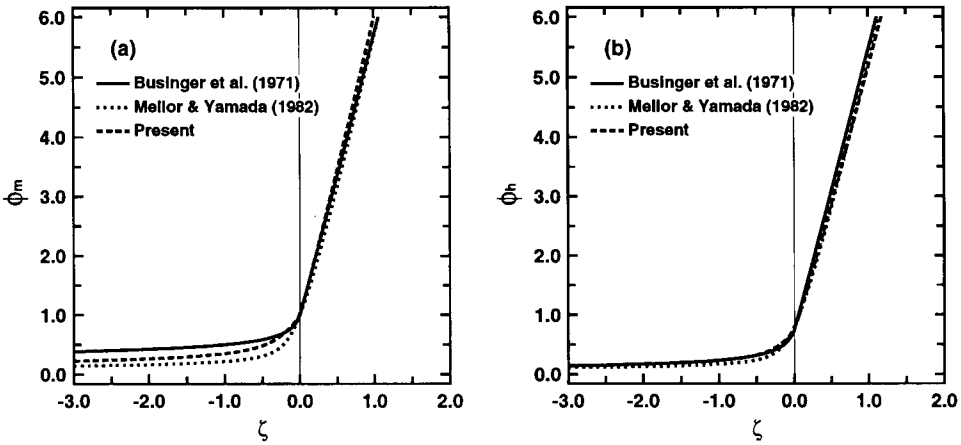

Figure 6. Comparison of the predicted (a) ϕ_m and (b) ϕ_h with the empirical functions. Dotted lines represent the results of the original M–Y model (Equation (9)), dashed lines those of the modified M–Y model (Equation (37)), and solid lines the empirical functions by Businger et al. (1971).

5.2. S_M AND S_H

Secondly, we will compare the non-dimensional eddy-diffusivity coefficients for momentum and heat, $S_M \equiv S_{M2.5} + S'_M$ and $S_H \equiv S_{H2.5} + S'_H$, in the modified M–Y model with those in the LES. S_M and S_H in the M–Y model are derived from Equations (29) and (30) after all the physical quantities, including L, are given by the LES data. Note that L given by Equations (38)–(41) nearly coincides with the LES results. S_M and S_H in the LES, on the other hand, are calculated from

$$S_M = \frac{\left(\langle uw\rangle^2 + \langle vw\rangle^2\right)^{1/2}}{Lq\left[(\partial U/\partial z)^2 + (\partial V/\partial z)^2\right]^{1/2}}, \tag{42}$$

$$S_H = -\frac{\langle w\theta\rangle}{Lq\,(\partial\Theta/\partial z)}. \tag{43}$$

Figure 7 shows vertical profiles of S_M in the modified M–Y model and the LES. Here, for the stable cases (Figures 7a–c), S_M in the M–Y model is estimated from the Level 2.5 model in which the turbulent diffusion of the temperature variance is neglected ($S'_M = 0$). This is because the temperature variance and/or its turbulent transport in these cases seem to be a little unsteady as will be shown later (Figures 11a–c) and consequently S'_M cannot be estimated properly. S_M in the modified M–Y model agrees fairly well with the LES results except near the centre of the PBL for Case 4 (Figure 7d), for which S_M in the LES seems to be large compared with that for Cases 5 and 6 (Figures 7e and f). If one looks at the figure more carefully, however, one notices that S_M near the surface in the LES for the stable cases is somewhat large (Figures 7a–c). This may be because physical quantities near the surface vary significantly with height and consequently the evaluation of

the denominators in Equation (42) becomes inaccurate. Also, for the unstable cases (Figures 7d–f), S_M in the modified M–Y model becomes larger than that in the LES as stability decreases, partly because ϕ_m in the M–Y model for $\zeta < 0$ is smaller than the empirical function (see Figure 6a).

Figure 8 shows vertical profiles of S_H as in Figure 7. For the stable cases (Figures 8a–c), S_H in the M–Y model is also estimated from the Level 2.5 model ($S'_H = 0$). S_H in the modified M–Y model nearly coincides with the LES results. For the stable cases (Figures 8a–c), however, S_H in the LES is generally larger than that in the modified M–Y model, partly because ϕ_h in the LES for $\zeta > 0$ is smaller than the empirical function (see Figure 2b). In the unstable cases (Figure 8d–f), S_H above the middle of the PBL is negative, illustrating that the upper part of the PBL has the structure of the countergradient diffusion. The absolute value of S_H near the centre of the PBL in the modified M–Y model becomes larger than that in the LES as stability decreases.

In order to demonstrate that the present modification of the closure constants leads to the improvement of the M–Y model, Figure 9 shows vertical profiles of S_M computed from the original M–Y model. Clearly, S_M in the original M–Y model (dashed line) is excessively large in the bulk of the convective PBL (Figures 9d–f). To improve the M–Y model, Kantha and Clayson (1994) changed two closure constants, C_3 and C_5, in Equation (9) to 0.2 and 0.7, respectively. Their modification, however, makes only a little improvement on the M–Y model (not shown). Dotted lines represent S_M in the case of $C_2 = 0.65$, $C_3 = 0.2$, and $C_5 = 0.7$. The magnitude of S_M for the unstable cases is reduced to some degree, although S_M for the stable cases becomes slightly larger than that in the LES (Figures 9a–c).

Thus, the consideration of buoyancy effects on the pressure covariances is likely to be necessary for the improvement of the M–Y model. Also the adequate expression for L is indispensable for that improvement; if the diagnostic equation for L by Mellor and Yamada (1974) is used for the unstable cases, both the original and modified M–Y models predict the eddy-diffusivity coefficient LqS_M smaller than half the LES results (not shown). Note that, in that case, S_M as well as L becomes small because S_M also depends upon L (see Equations (27)–(31)). Since this small LqS_M decreases the production of the TKE, it can become even smaller and is considered to cause the problems pointed out by Sun and Ogura (1980).

5.3. S_q AND S_θ

Mellor (1973) parameterized the third moments, e.g., the turbulent transports of the TKE and the temperature variance, by assuming downgradient diffusion. It is mentioned, however, that the downgradient-diffusion assumption for them is inadequate in the convective PBL (e.g., Moeng and Wyngaard, 1989).

Since the parameterization for the third moments is not examined in the present study, we will only show the non-dimensional eddy-diffusivity coefficients for the

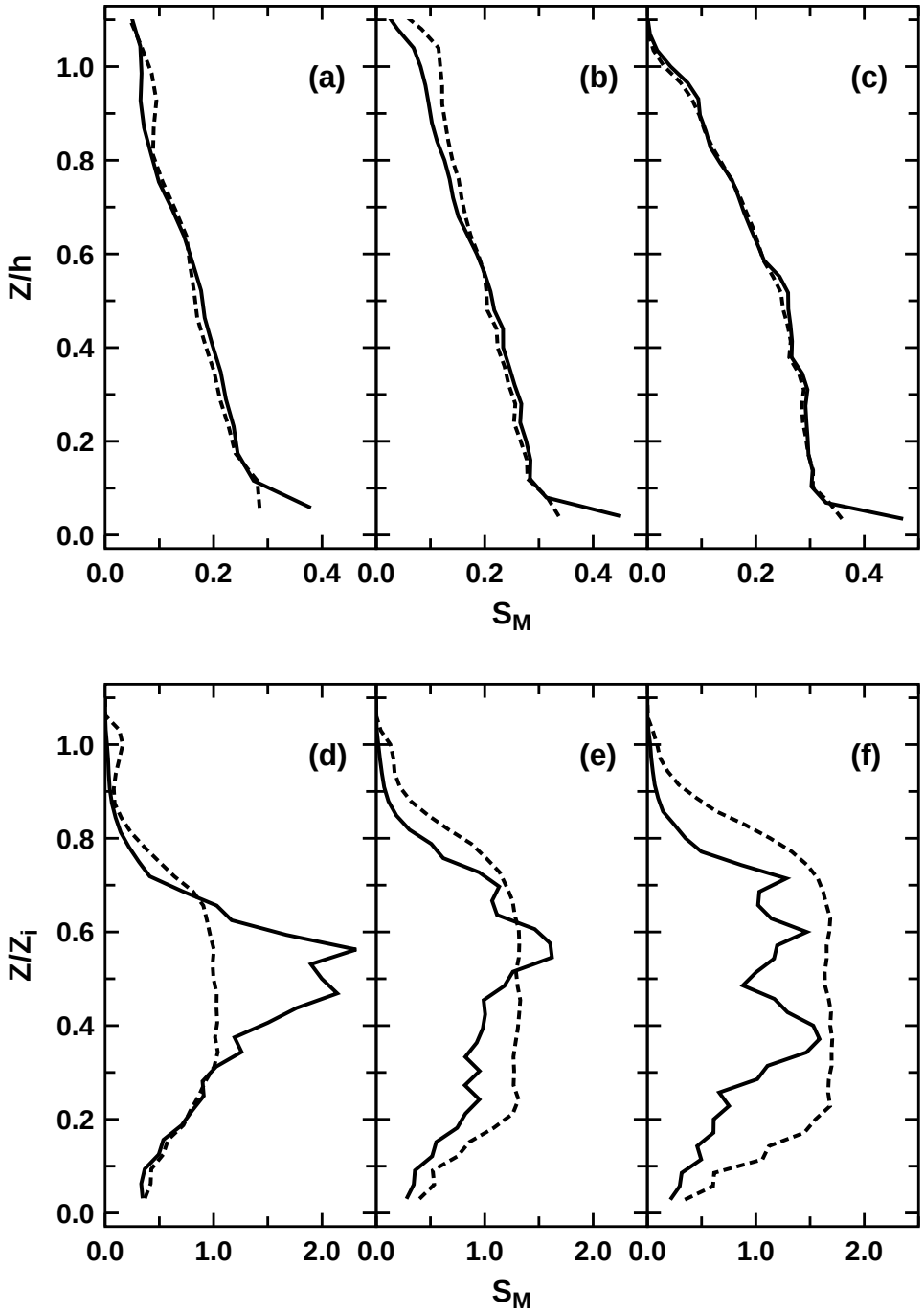

Figure 7. Comparison of S_M computed from the modified M–Y model (dashed line) with that from the LES data (solid line) for (a) Case 1, (b) Case 2, (c) Case 3, (d) Case 4, (e) Case 5, and (f) Case 6. The altitude is normalized as in Figure 5.

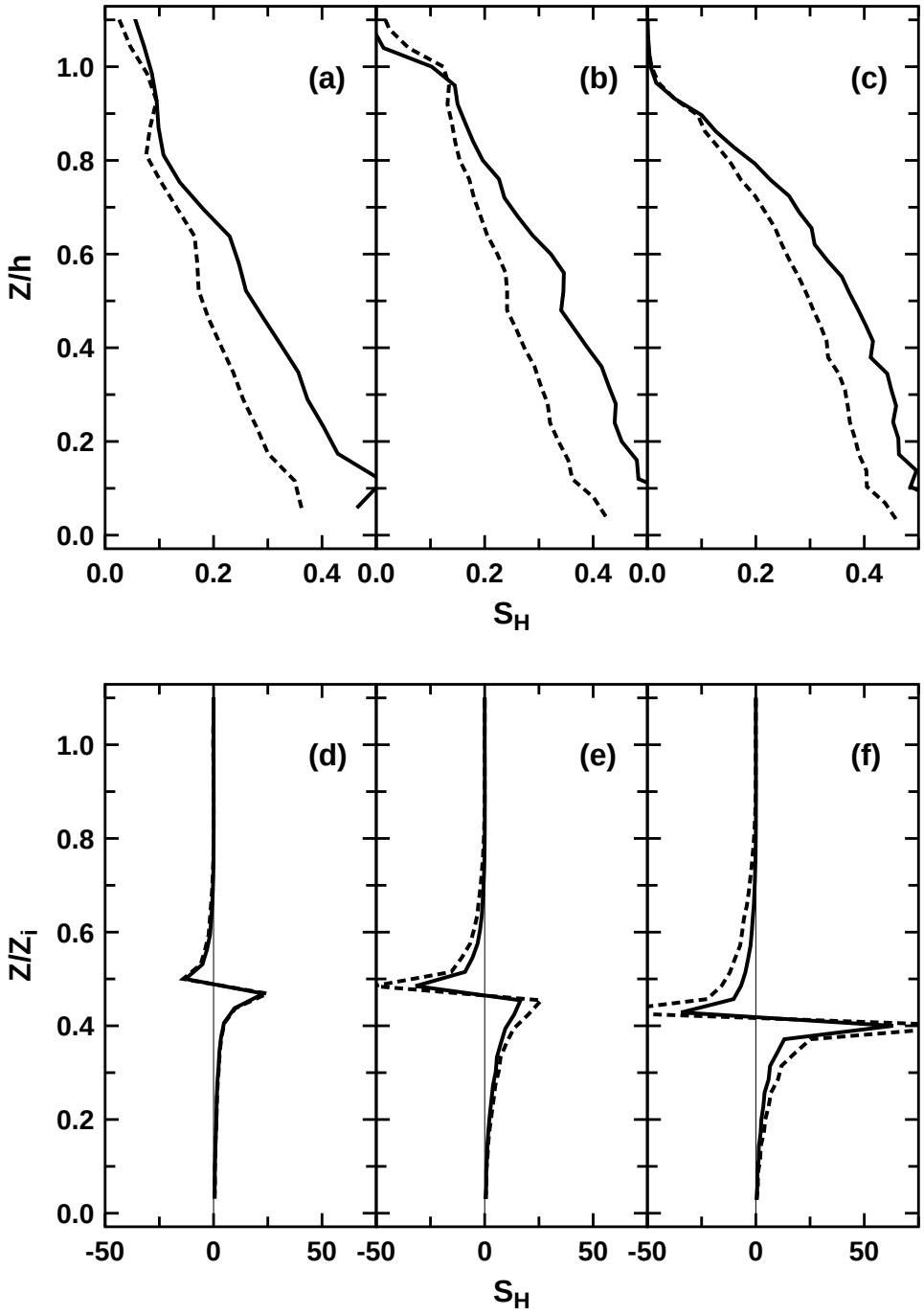

Figure 8. Same as Figure 7 except for S_H.

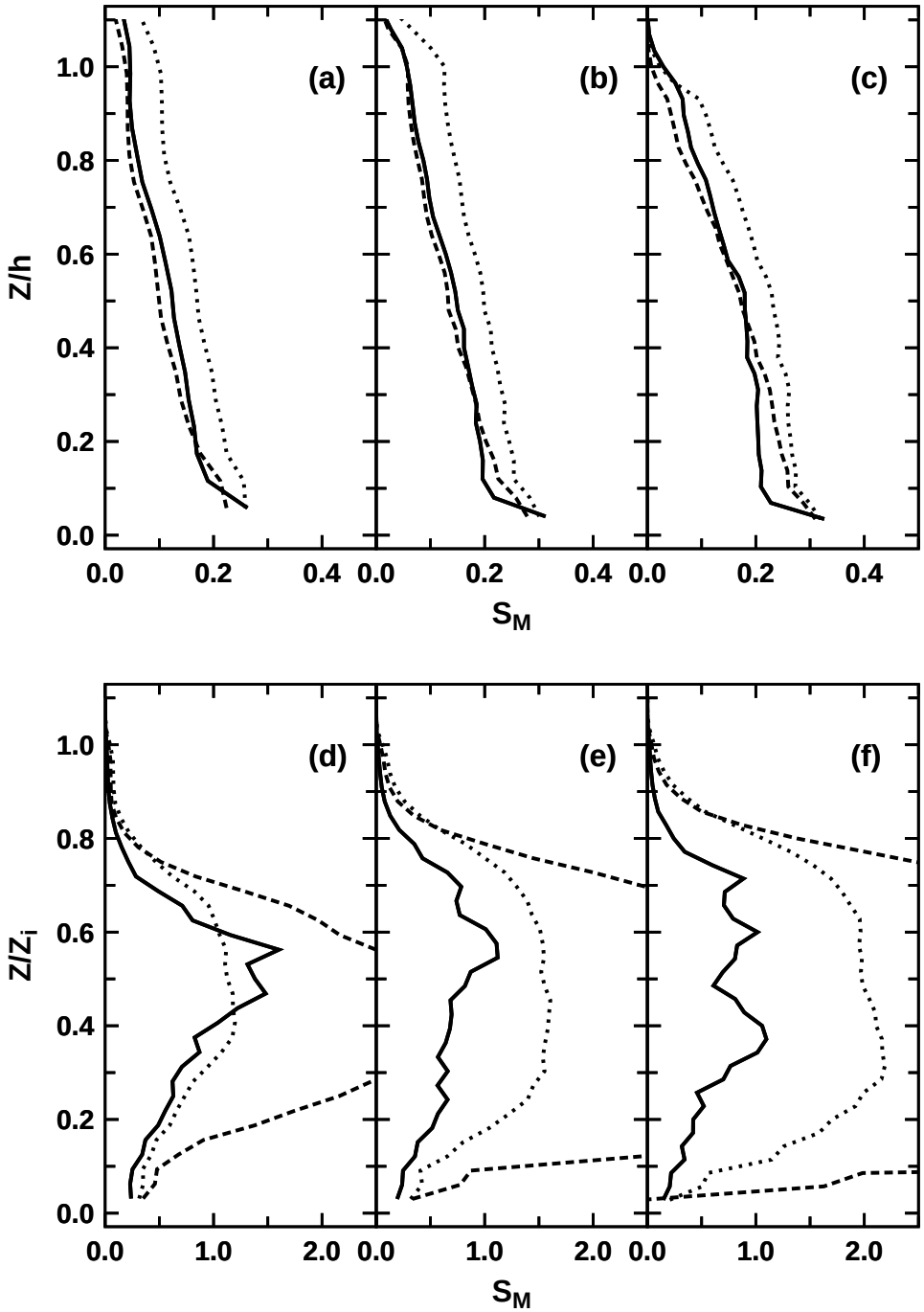

Figure 9. Same as Figure 7 except for S_M computed from the original M–Y model (dashed line). Dotted lines, however, represent S_M in the case of $C_2 = 0.65$, $C_3 = 0.2$, and $C_5 = 0.7$, where the last two values are the same as those of Kantha and Clayson (1994). Note that the magnitude of S_M from the LES data in this figure is smaller than that in Figure 7 because of the smaller value of B_1 and consequently a larger value of L.

TKE and the temperature variance, S_q and S_θ, similar to S_M and S_H. S_q and S_θ in the LES are calculated from

$$S_q = -\frac{\left\langle w(u^2+v^2+w^2)/2\right\rangle + \langle wp\rangle}{Lq\left[\partial(q^2/2)/\partial z\right]}, \tag{44}$$

$$S_\theta = -\frac{\left\langle w\theta^2\right\rangle}{Lq\left(\partial\langle\theta^2\rangle/\partial z\right)}, \tag{45}$$

where the subgrid turbulent transports are not included.

Figure 10 compares S_q with S_M computed from the LES data using Equation (42). S_q for the unstable cases is considerably larger than the constant value of 0.2 adopted by Mellor and Yamada (1982), except near the surface and the PBL top (Figures 10d–f), and becomes larger than S_M as stability decreases. Since such large values are considered to be unrealistic (e.g., Moeng and Wyngaard, 1989), it seems that the difference between S_q and S_M should be expressed in terms of the buoyancy flux as suggested by Therry and Lacarrère (1983).

Figure 11 compares S_θ with S_M. For the stable cases (Figures 11a–c), S_θ in the lower part of the PBL fluctuates largely, while S_θ in the upper part of the PBL is as small as S_M. Unlike S_q, S_θ for the unstable cases is nearly comparable with S_M except near $z/z_i = 0.7$ (Figures 11d–f). It seems that the turbulent transport of the temperature variance may be approximated based on the downgradient-diffusion assumption.

6. Summary and Conclusions

The M–Y turbulence closure model has several deficiencies that are common to almost all second-order closure models (e.g., Moeng and Wyngaard, 1989). We attempted to improve two of the deficiencies of the M–Y model.

To obtain a database for the improvement, stably-stratified and convective PBLs without moisture were simulated by a LES model (Nakanishi, 2000). Although LES is a well-established tool for the study of turbulent flows, the resulting data were compared with the empirical functions by Businger et al. (1971). The LES data reproduce the observed properties of the surface layer very well.

The first deficiency of the M–Y model is the neglect of buoyancy effects on the pressure covariances. We added the parameterization of its effects to the M–Y model, and presented a useful expression for the Level 3 model, and re-evaluated closure constants based on the LES data. The second deficiency is the uncertain expression for the master length scale L. We proposed a new diagnostic equation for L based on the LES data. The new equation allows L in the surface layer to vary with stability, and gives L in the upper part of the convective PBL with little underestimation.

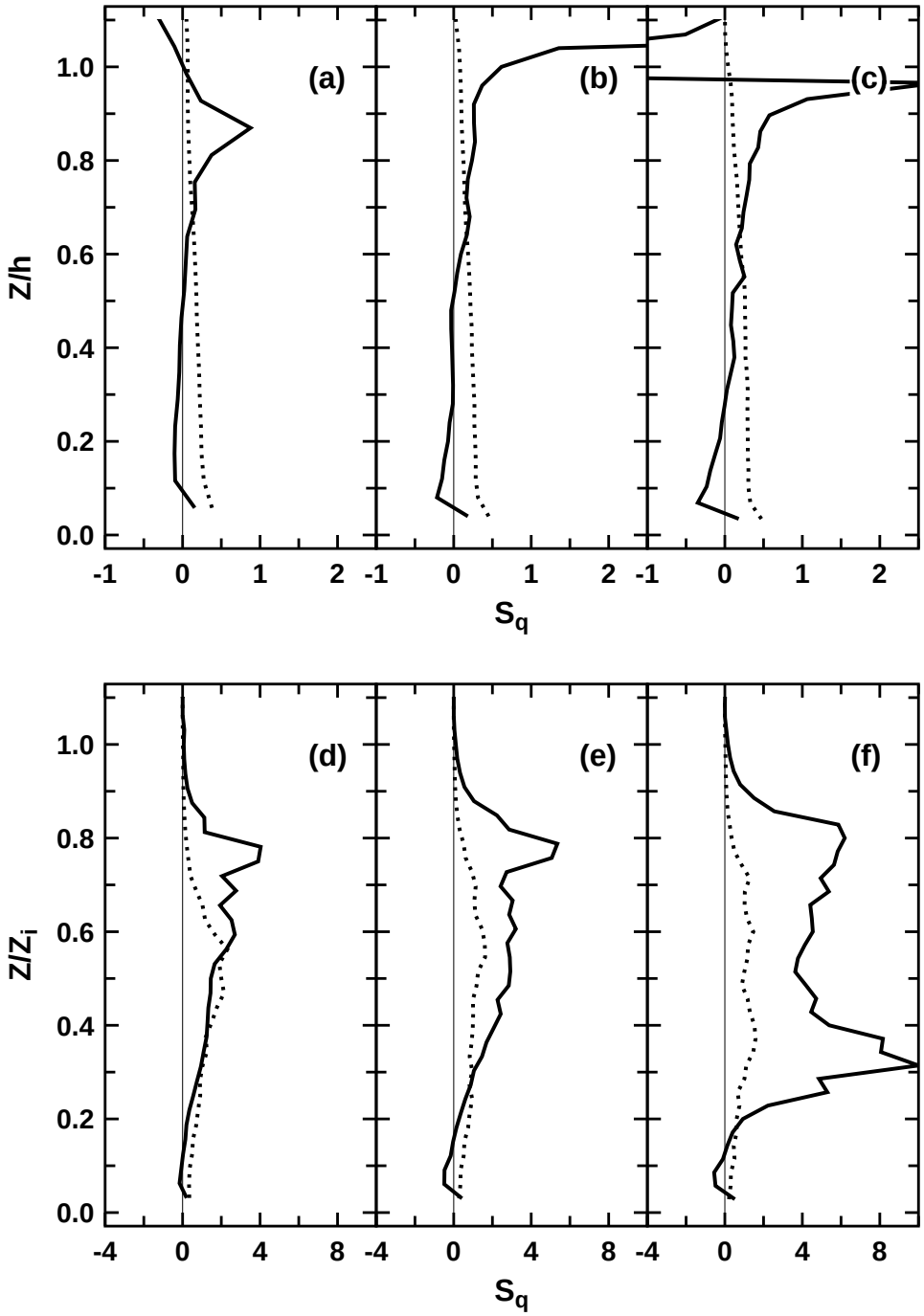

Figure 10. Vertical profiles of S_q (solid line) and S_M (dotted line) computed from the LES data for (a) Case 1, (b) Case 2, (c) Case 3, (d) Case 4, (e) Case 5, and (f) Case 6. The altitude is normalized as in Figure 5.

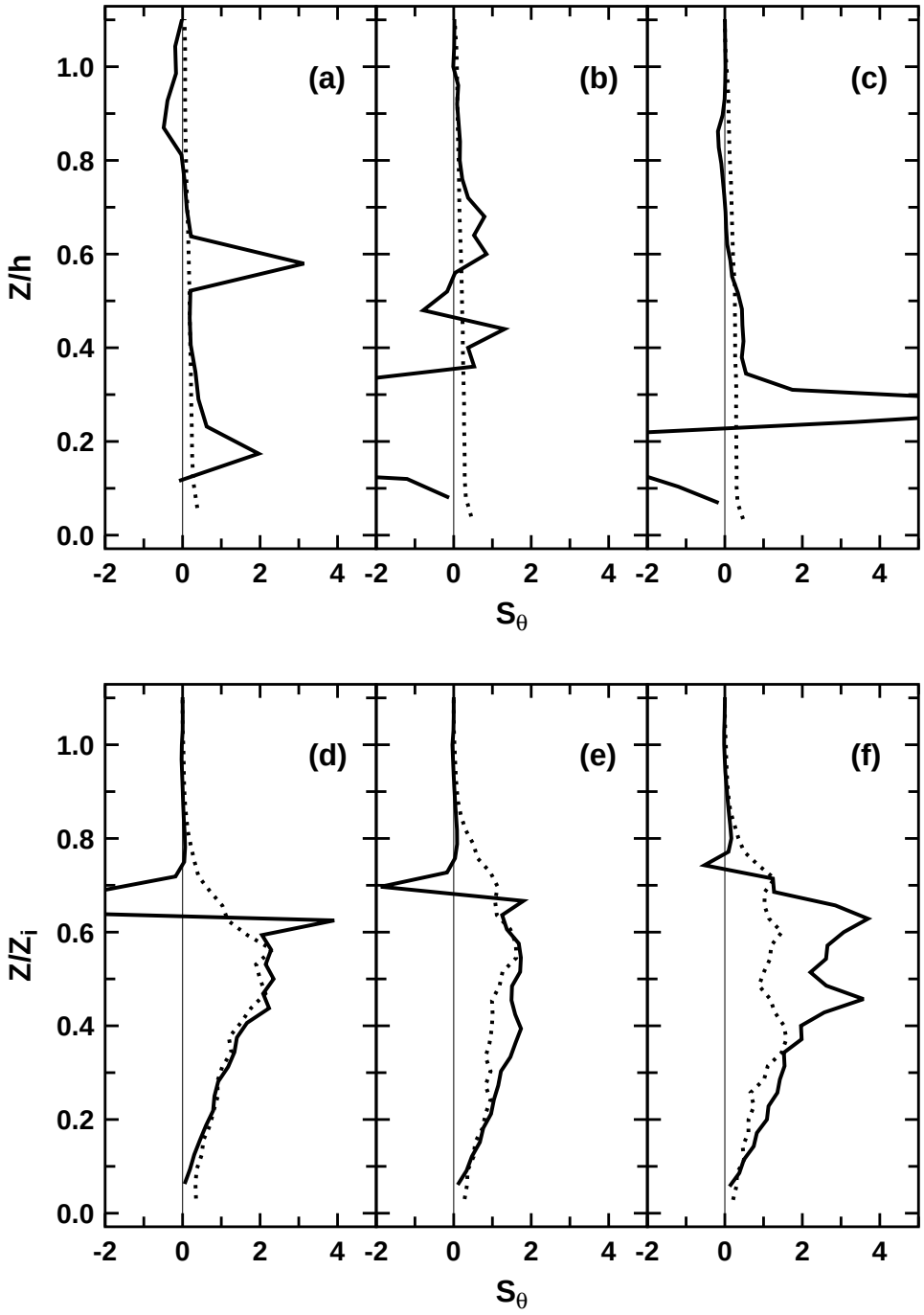

Figure 11. Same as Figure 10 except for S_θ.

The non-dimensional eddy-diffusivity coefficients for momentum and heat, computed from the modified M–Y model, agree well with those from the LES data. Such agreement is not obtained from the original M–Y model. The improvement is achieved by incorporating buoyancy effects into the parameterization for the pressure covariances and by using an adequate expression, such as our new diagnostic equation, for L.

The parameterization for the third moments, which is also important for turbulence closure modelling, was not discussed in the present paper. For reference, however, the non-dimensional eddy-diffusivity coefficients for the TKE and the temperature variance, S_q and S_θ, were compared with that for momentum, S_M. It is found that S_θ is nearly comparable with S_M, although S_q needs to be parameterized by considering buoyancy effects.

The performance of the modified M–Y model is expected to be satisfactory in a clear PBL. In a real PBL, however, moisture exists, and cloud and fog appear through its condensation. We have carried out the simulation of a radiation fog with the LES model (Nakanishi, 2000). We are now examining the performance of the modified M–Y model against the LES data on the radiation fog.

Acknowledgement

The author wishes to express his sincere thanks to Prof. H. Niino, Ocean Research Institute, the University of Tokyo, for his valuable suggestions and discussions and for his helpful comments on the manuscript.

Appendix A. Non-Dimensional Gradient Functions by Businger et al. (1971)

Based on the Kansas data, Businger et al. (1971) determined the non-dimensional gradient functions for momentum and heat, ϕ_m and ϕ_h, as

$$\phi_m = \begin{cases} 1 + 4.7\zeta, & \zeta \geq 0 \\ (1 - 15\zeta)^{-1/4}, & \zeta < 0, \end{cases} \tag{A1}$$

$$\phi_h = \begin{cases} Pr + 4.7\zeta, & \zeta \geq 0 \\ Pr\left[1 - 9(Pr/0.74)^2\zeta\right]^{-1/2}, & \zeta < 0, \end{cases} \tag{A2}$$

where the turbulent Prandtl number Pr is estimated to be 0.74.

Appendix B. Level 2 Model

In the Level 2 model (Mellor and Yamada, 1974, 1982), turbulent motions are assumed to be in a local-equilibrium state and all turbulent variables are solved diagnostically.

The equation for the TKE in a local-equilibrium state (Equation (16)) is written as

$$1 = B_1 (G_M S_{M2} + G_H S_{H2}) = B_1 G_M S_{M2} (1 - \mathrm{Rf}) \tag{B1}$$

with similar notations in Equation (27), where Rf is the flux Richardson number. By eliminating G_M and G_H from Equation (28) using the above equation, the non-dimensional eddy-diffusivity coefficients for momentum and heat, S_{M2} and S_{H2}, in the Level 2 model are obtained as

$$S_{M2} = \frac{A_1 F_1}{A_2 F_2} \frac{R_{f1} - \mathrm{Rf}}{R_{f2} - \mathrm{Rf}} S_{H2}, \tag{B2}$$

$$S_{H2} = 3A_2(\gamma_1 + \gamma_2) \frac{\mathrm{Rf}_c - \mathrm{Rf}}{1 - \mathrm{Rf}}, \tag{B3}$$

where

$$\begin{aligned} &\gamma_2 = 2A_1(3 - 2C_2)/B_1 + B_2(1 - C_3)/B_1, \\ &F_1 = B_1(\gamma_1 - C_1) + 2A_1(3 - 2C_2) + 3A_2(1 - C_2)(1 - C_5), \\ &F_2 = B_1(\gamma_1 + \gamma_2) - 3A_1(1 - C_2), \\ &R_{f1} = B_1(\gamma_1 - C_1)/F_1, \\ &R_{f2} = B_1\gamma_1/F_2, \end{aligned} \tag{B4}$$

and Rf_c is the critical flux Richardson number given by

$$\mathrm{Rf}_c = \frac{\gamma_1}{\gamma_1 + \gamma_2}. \tag{B5}$$

These expressions can be also obtained from Equations (23) and (24). S_{M2} and S_{H2} are characterized by not depending upon histories of the TKE and the master length scale, which exist in G_M and G_H.

The flux Richardson number Rf can be expressed in terms of the gradient Richardson number, $\mathrm{Ri} \equiv -G_H/G_M = \mathrm{Rf}\, S_{M2}/S_{H2}$, as

$$\mathrm{Rf} = R_{i1} \left[\mathrm{Ri} + R_{i2} - (\mathrm{Ri}^2 - R_{i3}\mathrm{Ri} + R_{i2}^2)^{1/2} \right], \tag{B6}$$

where

$$R_{i1} = \frac{1}{2} \frac{A_2 F_2}{A_1 F_1}, \quad R_{i2} = \frac{1}{2} \frac{R_{f1}}{R_{i1}}, \quad R_{i3} = \frac{2R_{f2} - R_{f1}}{R_{i1}}. \tag{B7}$$

Appendix C. Diagnostic Equation by Therry and Lacarrère (1983)

Based on the dissipation length scale L_ε obtained from field observation, laboratory experiment, and simulation, Therry and Lacarrère (1983) proposed a diagnostic equation for L_ε:

$$\frac{1}{L_\varepsilon} = \frac{1}{kz} + \frac{C_{e1}}{H} - \left(\frac{1}{kz} + \frac{C_{e2}}{H}\right) m_1 m_2 + \frac{C_{e5}}{L_b}, \tag{C1}$$

where

$$m_1 = 1/(1 + C_{e3} H/kz), \tag{C2}$$

$$m_2 = \begin{cases} 0, & \zeta \geq 0 \\ 1/(1 - C_{e4} L_M/H), & \zeta < 0, \end{cases} \tag{C3}$$

$$\frac{1}{L_b} = \begin{cases} N/(q^2/2)^{1/2}, & \partial\Theta/\partial z > 0 \\ 0, & \partial\Theta/\partial z \leq 0. \end{cases} \tag{C4}$$

H is the PBL depth given by

$$H = \begin{cases} 0.3u_*/f, & \zeta \geq 0 \\ z_i, & \zeta < 0, \end{cases} \tag{C5}$$

where f is the vertical component of the Coriolis parameter. The set of the constants is

$$(C_{e1}, C_{e2}, C_{e3}, C_{e4}, C_{e5}) = (15.0, 5.0, 0.005, 1.0, 1.5). \tag{C6}$$

References

Andrén, A.: 1991, 'A TKE-Dissipation Model for the Atmospheric Boundary Layer', *Boundary-Layer Meteorol.* **56**, 207–221.

Andrén, A.: 1995, 'The Structure of Stably Stratified Atmospheric Boundary Layers: A Large-Eddy Simulation Study', *Quart. J. Roy. Meteorol. Soc.* **121**, 961–985.

Andrén, A. and Moeng, C.-H.: 1993, 'Single-Point Closures in a Neutrally Stratified Boundary Layer', *J. Atmos. Sci.* **50**, 3366–3379.

Beljaars, A. C. M. and Holtslag, A. A. M.: 1991, 'Flux Parameterization over Land Surfaces for Atmospheric Models', *J. Appl. Meteorol.* **30**, 327–341.

Busch, N. E. and Larsen, S. E.: 1972, 'Spectra of Turbulence in the Atmospheric Surface Layer', in Risø Report No. 256, pp. 187–207.

Businger, J. A., Wyngaard, J. C., Izumi, Y., and Bradley, E. F.: 1971, 'Flux-Profile Relationships in the Atmospheric Surface Layer', *J. Atmos. Sci.* **28**, 181–189.

Canuto, V. M. and Minotti, F.: 1993, 'Stratified Turbulence in the Atmosphere and Oceans: A New Subgrid Model', *J. Atmos. Sci.* **50**, 1925–1935.

Deardorff, J. W.: 1972, 'Numerical Investigation of Neutral and Unstable Planetary Boundary Layers', *J. Atmos. Sci.* **29**, 91–115.

Denby, B.: 1999, 'Second-Order Modelling of Turbulence in Katabatic Flows', *Boundary-Layer Meteorol.* **92**, 67–100.

Dubrulle, B. and Niino, H.: 1992, 'On a Diagnostic Equation for a Turbulent Length Scale', in preprint, *Autumn Conference of Japan Meteorological Society*, Sapporo, 7–9 October 1992, Japan Meteorological Society, pp. 214–214 (in Japanese).

Gambo, K.: 1978, 'Notes on the Turbulence Closure Model for Atmospheric Boundary Layers', *J. Meteorol. Soc. Japan* **56**, 466–480.

Gerrity, J. P., Black, T. L., and Treadon, R. E.: 1994, 'The Numerical Solution of the Mellor–Yamada Level 2.5 Turbulent Kinetic Energy Equation in the Eta Model', *Mon. Wea. Rev.* **122**, 1640–1646.

Helfand, H. M. and Labraga, J. C.: 1988, 'Design of a Nonsingular Level 2.5 Second-Order Closure Model for the Prediction of Atmospheric Turbulence', *J. Atmos. Sci.* **45**, 113–132.

Kantha, L. H. and Clayson, C. A.: 1994, 'An Improved Mixed Layer Model for Geophysical Applications', *J. Geophys. Res.* **99(C12)**, 25,235–25,266.

Lewellen, W. S. and Teske, M. E.: 1973, 'Prediction of the Monin–Obukhov Similarity Functions from an Invariant Model of Turbulence', *J. Atmos. Sci.* **30**, 1340–1345.

Mellor, G. L.: 1973, 'Analytic Prediction of the Properties of Stratified Planetary Surface Layers', *J. Atmos. Sci.* **30**, 1061–1069.

Mellor, G. L. and Yamada, T.: 1974, 'A Hierarchy of Turbulence Closure Models for Planetary Boundary Layers', *J. Atmos. Sci.* **31**, 1791–1806.

Mellor, G. L. and Yamada, T.: 1982, 'Development of a Turbulence Closure Model for Geophysical Fluid Problems', *Rev. Geophys. Space Phys.* **20**, 851–875.

Miyakoda, K., Gordon, T., Caverly, R., Stern, W., Sirutis, J., and Bourke, W.: 1983, 'Simulation of a Blocking Event in January 1977', *Mon. Wea. Rev.* **111**, 846–869.

Moeng, C.-H. and Sullivan, P. P.: 1994, 'A Comparison of Shear- and Buoyancy-Driven Planetary Boundary Layer Flows', *J. Atmos. Sci.* **51**, 999–1022.

Moeng, C.-H. and Wyngaard, J. C.: 1986, 'An Analysis of Closures for Pressure-Scalar Covariances in the Convective Boundary Layer', *J. Atmos. Sci.* **43**, 2499–2513.

Moeng, C.-H. and Wyngaard, J. C.: 1988, 'Spectral Analysis of Large-Eddy Simulations of the Convective Boundary Layer', *J. Atmos. Sci.* **45**, 3573–3587.

Moeng, C.-H. and Wyngaard, J. C.: 1989, 'Evaluation of Turbulent Transport and Dissipation Closures in Second-Order Modeling', *J. Atmos. Sci.* **46**, 2311–2330.

Nakanishi, M.: 2000, 'Large-Eddy Simulation of Radiation Fog', *Boundary-Layer Meteorol.* **94**, 461–493.

Niino, H.: 1990, 'On the Prognostic Equation for the Turbulent Master Length Scale in a Turbulence Closure Model', in preprint, *Spring Conference of Japan Meteorological Society*, Tokyo, 23–25 May 1990, Japan Meteorological Society, pp. 215–215 (in Japanese).

Numerical Prediction Division of Japan Meteorological Agency: 1997, *Outline of the Operational Numerical Weather Prediction at the Japan Meteorological Agency*, Japan Meteorological Agency, Tokyo, 126 pp.

Schumann, U.: 1977, 'Realizability of Reynolds Stress Turbulence Models', *Phys. Fluids* **20**, 721–725.

Sullivan, P. P., McWilliams, J. C., and Moeng, C.-H.: 1994, 'A Subgrid-Scale Model for Large-Eddy Simulation of Planetary Boundary-Layer Flows', *Boundary-Layer Meteorol.* **71**, 247–276.

Sun, W.-Y. and Ogura, Y.: 1980, 'Modeling the Evolution of the Convective Planetary Boundary Layer', *J. Atmos. Sci.* **37**, 1558–1572.

Therry, G. and Lacarrère, P.: 1983, 'Improving the Eddy Kinetic Energy Model for Planetary Boundary Layer Description', *Boundary-Layer Meteorol.* **25**, 63–88.

Yaglom, A. M.: 1977, 'Comments on Wind and Temperature Flux-Profile Relationships', *Boundary-Layer Meteorol.* **11**, 89–102.

Yamada, T.: 1977, ‘A Numerical Experiment on Pollutant Dispersion in a Horizontally-Homogeneous Atmospheric Boundary Layer’, *Atmos. Environ.* **11**, 1015–1024.